Time-Resolved Resonance Raman and Density Functional Study of the Radical Cation of Promazine

ARTICLE *in* THE JOURNAL OF PHYSICAL CHEMISTRY A · AUGUST 1999

Impact Factor: 2.69 · DOI: 10.1021/jp991342y

3 AUTHORS, INCLUDING:

Lian C T Shoute
University of Alberta
58 PUBLICATIONS **891** CITATIONS

SEE PROFILE

David Lee Phillips
The University of Hong Kong
345 PUBLICATIONS **7,051** CITATIONS

SEE PROFILE

Time-Resolved Resonance Raman and Density Functional Study of the Radical Cation of Promazine

Duohai Pan, Lian C. T. Shoute,† and David Lee Phillips*

Department of Chemistry, University of Hong Kong, Pokfulam Road, Hong Kong

Received: April 26, 1999; In Final Form: July 1, 1999

We present a resonance Raman spectrum of the radical cation of promazine. Density functional theory computations were used to find the structures, hyperfine coupling constants (hfcc's), spin densities, and vibrational frequencies for the ground electronic states of the neutral promazine molecule and its radical cation. Preliminary assignments for all of the observed Raman bands for the neutral promazine molecule and its radical cation are given. The density functional theory computed optimized structures show the S_0 states of the neutral molecule (with a dihedral angle of 147.1°) and its radical cation (with a dihedral angle of 172.13°) are both nonplanar. The DFT-computed spin densities suggest the radical cation of promazine has significantly more spin density on nitrogen compared to sulfur, while the sulfur has a greater spin density than nitrogen in the radical cation of phenothiazine. The calculated HOMO and LUMO electron densities display noticeable differences in both the central ring and the side chain upon excitation. This appears consistent with the promazine radical cation experimental resonance Raman intensities.

Introduction

Phenothiazine derivatives with an *N*-aminopropyl side chain and/or a variety of ring substituents such as promazine and chloropromazine have been attractive subjects for research because of their applications as neuroleptic agents and tranquilizers.[1−4] Phenothiazine and its derivatives are also of interest because of their potential use in solar energy applications.[5] Previous studies on phenothiazine, promazine and chloropromazine tranquilizers suggested that these compounds act as good electron donors and can function as a charge transfer or electron transfer donor at drug receptor sites.[6] This hypothesis is consistent with the observation of the formation of charge-transfer complexes of phenothiazines and its derivatives with a variety of acceptor compounds.[7] Phenothiazine and its derivatives such as promazine can also form relatively stable radical cations. It has been suggested that these radical cations are important in the biological function of phenothiazine compounds.[8] Since phenothiazine drugs are very sensitive to changes in molecular structure, it is important to elucidate detailed information about the geometry and electronic structure of these substances in order to better understand how small changes in the molecules can affect the biological activities.

Photoelectron spectra of phenothiazine and four biologically active derivatives (e.g., promazine, chlorpromazine, thioridazine, and trifluoperazine) were obtained by Houk and co-workers.[10] They found that the first ionization potential is N-centered and the second ionization potential is S-centered for all of the compounds. They also found very little variation in the ionization potential among the five compounds studied, and this suggests that there is not a direct relationship between the ionization potential and the neuroleptic activity in the limited series of phenothiazine compounds examined.[10] The biological activities of phenothiazine compounds appear to be related to the ability of the aromatic moiety to form a molecular complex at the receptor site, and this depends on the particular side chain substituent of the phenothiazine derivative; results of several EPR studies support this idea.[11,12] Time-resolved absorption spectroscopy experiments for promazine and chlorpromazine found that the radical cation is formed via a direct photoionization mechanism (mostly by a two-photon process) and chlorpromazine radical via loss of the chlorine atom from the triplet state.[13] Because chlorpromazine is about an order of magnitude more toxic than promazine[14] and a multiphoton process is not expected under ambient conditions, the photoreactivity of these compounds was ascribed to the formation of the radical by dechlorination of chlorpromazine. Time-resolved absorption and fluorescence investigations of reactions of phenothiazine and some of its derivatives with chloroalkanes found that an electron transfer or charge transfer interaction occurs when the radical cation is present.[15]

X-ray diffraction work on crystals of phenothiazine and its derivatives found that the molecular structures are dependent on the side chain and other substituents attached to the phenothiazine moiety.[16] The neutral phenothiazine molecule is folded about the N−S axis with two planes of the rings having a dihedral angle of 158.5° and this dihedral angle changes substantially for promazine (∼140°) and chlorpromazine (∼139°). Phenothiazine and its derivatives have been found to open their structures noticeably upon formation of their radical cations. The results of photoionization studies suggested the amine part of phenothiazine is pyramidal in the neutral ground electronic state and planar in the radical cation ground electronic state.[10] This interpretation is consistent with EPR experiments for the radical cation of phenothiazine[17] as well as with our recent ab initio DFT calculations and experimental Raman spectra for phenothiazine.[18] EPR spectra indicated that the radical cations of promazine and chlorpromazine are nonplanar and the folding dihedral angle of chlorpromazine radical cation was estimated to be ∼169.9°.[11]

Resonance Raman and time-resolved resonance Raman investigations have been reported for phenthiazine and its photo-

* Author to whom correspondence should be addressed.
† Present address: Department of Chemistry, University of Saskatchewan, Saskatoon, Canada S7N 0W0.

10.1021/jp991342y CCC: $18.00
Published on Web 08/07/1999

chemical reactions.[18−20] Takahashi and co-workers have used nanosecond time-resolved resonance Raman spectroscopy to study the triplet state and radical cation of phenothiazine and 2-chlorphenothiazine.[20] Their results indicated that the spin density is localized on the S atom in the T_1 state. A Raman and ab initio density functional theory (DFT) study on phenothiazine and its radical cation found that the neutral phenothiazine in its ground electronic state has a nonplanar structure with a dihedral angle ∼153°, while the radical cation has a planar (or nearly planar) structure with a dihedral angle of ∼180°.[18] The Raman spectra and the electronic structure calculations[18] suggest that the HOMO of the phenthiazine radical cation is a π-bonding orbital localized on the S and N atoms and the LUMO electron density is mainly antibonding π*-orbital in character.[18]

In this paper, we report a resonance Raman spectrum of the radical cation of promazine. We have carried out additional FT-Raman experiments for the ground state of the neutral promazine molecule and have done ab initio [both Hartee−Fock (HF) and density functional theory (DFT)] calculations for both neutral promazine and its radical cation in their ground electronic states. The optimized structure, electron spin distribution, and vibrational frequencies of the neutral promazine molecule and its radical cation were obtained from the ab initio calculations. We have made preliminary vibrational assignments for the experimental vibrational frequencies observed for promazine and its radical cation. The structural and vibrational frequency changes observed upon formation of the radical cation from the neutral parent molecule are discussed in conjunction with the calculated electronic structures. We compare our current results for the radical cations of promazine with previous results for phenothiazine and discuss their differing structures and biological activities.

Experiment

The apparatus and methods used to obtain experimental nanosecond time-resolved resonance Raman spectra have been previously reported, so we shall just provide a short description here.[21−23] The hydrogen Raman shifted laser lines of the third harmonic (355 nm) of a nanosecond pulsed Nd:YAG laser provided the pump (309.1 nm) and probe (502.9 nm) wavelengths used for the time-resolved resonance Raman experiments. The pump and probe pulses were delayed using a 15 ns optical delay. A near collinear geometry was used to lightly focus the pump and probe laser beams onto a flowing liquid sample, and a backscattering geometry was used to collect the Raman scattered light. The Raman light signal was then imaged through a depolarizer, and the entrance slits of a double monochromator (0.22 m from CVI). The gratings of the double monochromator then dispersed the Raman light signal onto a CCD detector which collected the signal before reading the signal out to a PC computer. Approximately 10−15 readouts (with 60 × 10 s scans each) were added together to get the resonance Raman spectrum. The FT-Raman spectra of the neutral promazine molecule in its ground electronic state were taken with a commercial FT-Raman spectrometer (Bio-Rad) using 1064 nm cw excitation.

Promazine and spectroscopic grade methanol and carbon tetrachloride were purchased from Aldrich and used to prepare samples for the Raman experiments. Samples with concentrations of $\sim 6 \times 10^{-3}$ M promazine dissolved in a 10:3 methanol/CCl_4 mixed solvent were used in the time-resolved resonance Raman experiments. The mixed solvent system helped to quench the promazine fluorescence and triplet state and made it easier to produce the radical cation of promazine. Laser photolysis

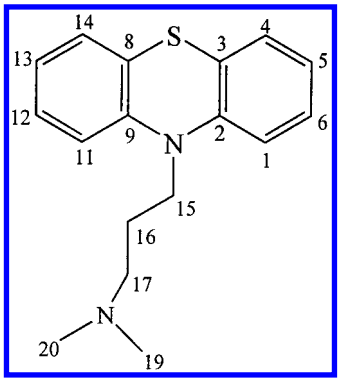

Figure 1. Diagram of the promazine molecule with the carbon and nitrogen atoms numbered 1−20.

experiments showed that the promazine radical cation is promptly formed and has an absorption band ∼510 nm with a ∼100 μs lifetime.[13] The transient absorption of 510 nm is close to the 502.9 nm probe excitation wavelength used in our time-resolved resonance Raman experiments to probe the promazine radical cation. An investigation of the photoinduced interaction of phenothiazines with chloroalkanes showed that no exciplex between the phenothiazines and chloroalkane in polar solvent/CCl_4 solvent systems.[15] The transient resonance Raman spectrum of the radical cation of phenothiazine in pure methanol solvent is almost the same as the spectrum obtained in a methanol/CCl_4 mixed solvent system.[18,20] In addition, no new bands such as a C−Cl stretch mode (which is readily observed in the radical cation spectra of 2-chlorophenothiazine and chlorpromazine) are observed in the transient resonance Raman spectrum at different delay times for the radical cation spectra of promazine. Thus, we are reasonably confident that the observed transient resonance Raman spectra of the radical cation of promazine reported here does not have any noticeable interference from any chlorine intermediates.

Calculations

Density functional theory (DFT) calculations were performed using the Gaussian program suites (G94 was run on an IBM 9076 SP2 computer and G98 was run on a PC computer).[24] We computed the optimized structures, electron spin distribution, hyperfine splitting constants, and the vibrational frequencies of promazine and its radical cation. The DFT calculations were performed with Bechke's three-parameter hybrid method using the Lee−Yang−Parr correlation functional (B3LYP)[25] and the 6-31G* split-valence polarization basis set. The gradients and vibrational frequencies were found analytically. No imaginary frequency modes were observed at the optimized structures of the promazine neutral molecule or its radical cation. Descriptions of the different vibrational modes were formulated using the potential energy distributions (PED) found from the program NMODE[26] in conjunction with visual inspection of the animated normal mode found using the Molden program.[27] We calculated the isotopic shifts of the S^{34}- and N^{15}-substituted promzaine to help make some tentative vibrational assignments by comparison to isotopic data previously found for the structurally similar phenothiazine system. We also carried out Hartree−Fock (HF) calculations for the ground state of promazine using the Gaussian programs[24] for comparison with the DFT calculation results.

Results and Discussion

Figure 1 presents a simple schematic of the promazine molecule with the carbon and nitrogen atoms numbered 1−20,

TABLE 1: Structural Parameters for the Ground State of the Neutral Promazine Molecule Calculated Using HF and DFT Methods with a 6-31G* Basis Set and a Compariosn to Experimental Values Determined by X-ray Diffraction (Bond Lengths in Å, Bond Angles in Degrees)

parameters	RHF calcd	DFT/B3LYP calcd	X-ray expt[a]
dihedral angle (S−N)	145	147.1	140
dihedral ($C_{16}-C_{15}-N-C_2$)	84.335	82.167	
dihedral ($C_{17}-C_{16}-C_{15}-N$)	162.295	161.829	
dihedral ($C_{20}-N_{18}-C_{17}-C_{16}$)	82.501	81.237	
C_3-S-C_8	98.878	99.292	99
C_2-N-C_9	120.794	121.681	117
C_3-S	1.769	1.778	1.76
C_8-S	1.770	1.779	1.77
C_2-N	1.408	1.414	1.41
C_9-N	1.410	1.416	1.46
$C_{15}-N$	1.394	1.466	
C_1-C_2	1.384	1.407	
C_2-C_3	1.398	1.412	1.377
C_3-C_4	1.384	1.395	
C_4-C_5	1.384	1.395	1.39
C_5-C_6	1.380	1.391	1.36
C_6-C_1	1.386	1.396	
$C_{15}-C_{16}$	1.541	1.546	
$C_{16}-C_{17}$	1.531	1.536	
$C_{17}-N_{18}$	1.456	1.468	
$N_{18}-C_{19}$	1.449	1.459	
$N_{18}-C_{20}$	1.449	1.46	
C_1-H_1	1.069	1.081	
C_4-H_4	1.075	1.087	
C_5-H_5	1.074	1.086	
C_6-H_6	1.075	1.087	
C_2-N-C_{15}	119.518	118.667	
C_9-N-C_{15}	118.451	117.785	
C_2-C_3-S	119.909	120.414	
C_3-C_2-N	120.817	121.188	
$S-C_3-C_4$	118.852	118.297	
$C_2-C_1-H_1$	120.433	120.281	
$C_1-C_2-C_3$	117.187	117.047	
$C_2-C_3-C_4$	121.087	121.085	
$C_3-C_4-H_4$	118.848	118.710	
$C_3-C_4-C_5$	120.917	120.905	
$C_4-C_5-H_5$	120.397	120.278	
$C_4-C_5-C_6$	118.589	118.720	
$C_5-C_6-H_6$	120.324	120.434	
$C_5-C_6-C_1$	120.733	120.631	

[a] Values are from X-ray diffraction experimental results reported in ref 12.

TABLE 2: Structural Parameters for the Ground State of the Radical Cation of Promazine Calculated Using HF and DFT Methods with a 6-31G* Basis Set and a Comparison to Experimental Values Determined by X-ray Diffraction for Chlorpromazine (Bond Lengths in Å, Bond Angles in Degrees)

parameters	RHF calcd	DFT/B3LYP calcd	X-ray expt[a]
dihedral angle (S−N)	168.5	172.13	169.9
dihedral ($C_{16}-C_{15}-N-C_2$)	89.559	88.612	88.4
dihedral ($C_{17}-C_{16}-C_{15}-N$)	160.90	155.189	178.3
dihedral ($C_{20}-N_{18}-C_{17}-C_{16}$)	86.137	84.886	54.5
C_3-S-C_8	100.19	101.133	99.6
C_2-N-C_9	124.08	124.841	123.5
C_3-S	1.75	1.762	1.776
C_8-S	1.75	1.762	1.733
C_2-N	1.385	1.407	1.391
C_9-N	1.386	1.407	1.442
$C_{15}-N$	1.499	1.496	1.459
C_1-C_2	1.424	1.422	1.414
C_2-C_3	1.419	1.421	1.361
C_3-C_4	1.400	1.404	1.392
C_4-C_5	1.392	1.388	1.385
C_5-C_6	1.400	1.408	1.358
C_6-C_1	1.384	1.386	1.360
$C_{15}-C_{16}$	1.534	1.545	1.499
$C_{16}-C_{17}$	1.533	1.542	1.527
$C_{17}-N_{18}$	1.455	1.467	1.509
$N_{18}-C_{19}$	1.456	1.468	1.453
$N_{18}-C_{20}$	1.455	1.468	1.453
C_1-H_1	1.067	1.079	
C_4-H_4	1.074	1.084	
C_5-H_5	1.073	1.083	
C_6-H_6	1.073	1.084	
C_2-N-C_{15}	118.307	117.89	118.7
C_9-N-C_{15}	117.595	117.255	117.6
C_2-C_3-S	122.994	122.99	125.0
C_3-C_2-N	122.220	122.809	122.6
$S-C_3-C_4$	116.346	115.782	113.4
$C_2-C_1-H_1$	120.967	120.365	
$C_1-C_2-C_3$	117.869	117.023	117.6
$C_2-C_3-C_4$	120.076	121.203	121.5
$C_3-C_4-H_4$	118.796	119.180	
$C_3-C_4-C_5$	121.097	120.436	120.5
$C_4-C_5-H_5$	120.073	120.164	
$C_4-C_5-C_6$	119.366	119.316	117.3
$C_5-C_6-H_6$	120.385	120.305	
$C_5-C_6-C_1$	120.551	120.722	123.4

[a] Values are from X-ray diffraction expermental results reported in ref 11.

which corresponds to the numbering of these atoms in Tables 1 and 2. Table 1 presents the structural parameter results found from the DFT B3LYP/6-31G* and RHF/6-31G* computations and corresponding experimental results[12] for the ground electronic state of neutral promazine. The dihedral angles between the two lateral rings are 145.2° and 147.1° for the RHF and DFT computations, respectively, but only 140° for the X-ray experiment on promazine HCl crystals.[12] This discrepancy between the calculated and experimental results is probably due to some intermolecular interaction present in the experimental values of the maleate salt (e.g., packing of the molecules in the crstalline form may affect the dihedral angle found from the X-ray experiments on promazine salt). None the less, both experimental and calculated values for the dihedral angle show that the ground electronic state of promazine is folded along the N−S axis. The introduction of the $-(CH_2)_3N(CH_3)_2$ side chain at the N atom position of the phenothiazine group to form the promazine derivative leads to changes in the values of the dihedral angle from 152.2° for phenothiazine[18] to 147° for promazine (this work) as computed from DFT calculations, and the X-ray experiments are similar to 158.5 or 153.3° for phenothiazine[16,28] and 140° for promazine.[12] This implies the degree of folding increases for larger substituents at N-substituted derivatives such as promazine and chlorpromazine where the steric repulsions of the subsituted side chain forces an additional folding of the ring system.[11] Inspection of Table 1 shows the RHF and DFT calculations generally give similar values for the bond lengths and bond angles of the ground electronic state of promazine and show reasonable agreement with the corresponding experimental values. Hartree−Fock methods are believed to give C−H bond lengths for closed-shell molecules that are ∼0.01 Å too short,[29] so the DFT-calculated values likely provide better results for the C−H bond lengths. Comparison of the CSC and CNC bond angles of Table 1 for promazine with those found for phenothiazine[18] shows that the introduction of the side chain to phenothiazine at the N atom position has little or no effect on these bond angles.

Table 2 lists the structural parameters for the radical cation of promazine determined from UHF and DFT calculations. Although Soria and co-workers[11] reported a structural investigation of the promazine radical cation by EPR and X-ray

TABLE 3: Hyperfine Coupling Constants (hfcc's) Calculated Using DFT Methods with a 6-31G* Basis Set and a Comparison to Experimental Values for Phenothiazine (PHT) and Promazine (PRZ) Radical Cations (hfcc's in Gauss Units)

	DFT/B3LYP calcd		exptl	
parameter	PTH	PRZ	PTH[a]	PRZ[b]
$\alpha(N)$	5.45	9.414	6.34	7.08
$\alpha(\beta H)$	−7.94	3.53	7.29	3.52
$\alpha(H_1)$	0.744	−1.388	1.13	0.92
$\alpha(H_4)$	−0.982	0.942	0.5	0.4
$\alpha(H_5)$	−2.664	−2.837	2.49	1.92
$\alpha(H_6)$	−0.664	−0.2373	0.5	0.8
$\alpha(N)/\alpha(H_5)$	2.060	3.318	2.546	3.612

[a] Values from ref 17. [b] Values from ref 30.

diffraction, they were not able to determine quantitative structural parameters from this work. However, they were able to obtain quantitative results for the radical cation of chlorpromazine.[11] The triplet states of promazine and chlorpromazine behave very differently in various solvents,[13] but these compounds have very similar structures in the neutral and radical cations differing only in the chlorine atom. In the absence of quantitative structural information for the radical cation of promazine, we compare the results available for the radical cation of chlorpromazine[11] to our ab initio results for the radical cation of promazine in Table 2. We note that there is probably some perturbation of the radical cation of promazine by the chlorine atom in chlorpromazine, but we expect that their structures are similar to one another. The UHF and DFT calculations for promazine radical cation in Table 2 show that the dihedral angle is 168.5° (UHF) and 172.1° (DFT) and these values are close to the chlorpromazine value of 169°.[11] Comparison of the results of Tables 1 and 2 indicate that the folding about the N−S axis increases with oxidation. The DFT calculation results for promazine and its radical cation given in Tables 1 and 2 show that the dihedral angle increases in value from 147° for promazine to 172.1° in the promazine radical cation. It is interesting to note that the promazine radical cation is nonplanar but the phenothiazine radical cation is planar.[18] We also note that the qualitative results of an electron spin resonance (ESR) study found that the promazine radical cation is likely nonplanar.[30] The ESR investigations[11,12,30] suggest that oxidation affects the folding dihedral angle in two ways: a direct increase in the angle in both radical cations of phenothiazine and promazine due to the change in heteroatom hybridation and an indirect increase due to the decrease of the steric repulsions (absent in the radical cation of phenothiazine). When the repulsions are relaxed by oxidation (e.g., formation of the radical cation from the neutral molecule), a larger uniformity of folding angles occurs.

Table 3 compares ab initio calculated proton hyperfine coupling constants (hfcc's) with their corresponding experimental values for both phenothiazine and promazine radical cations. Since UHF and UMP2 ab initio methods are known to be deficient in calculating hfcc's and spin densities due to severe spin contamination of the ground state wave function,[29] we have only used the hybrid HF/DF (B3LYP) calculations to compare to the experimental values. Several studies on other organic radicals have shown that gradient-corrected BP86, BLYP, and hybrid HF/DF B3LYP methods give calculated hfcc's close to the values obtained from experimental ESR results.[31−33] Our DFT (B3LYP) results in Table 3 for the radical cation of promazine show a proton hfcc value for N of 9.414 G which is in reasonable agreement with the experimental value of $\alpha(N)$ (7.08 G). The calculated hfcc's values for βH (3.53 G) and H_1 (−1.388 G) are close to the values from ESR experiments (3.53 G and 0.92 G, respectively). We obtained similar agreement in Table 3 between our ab initio (DFT) calculated values and the ESR experimental values reported by Soria and co-workers[11] for the phenothiaine radical cation. We note that the ratios of the $\alpha(N)/\alpha(H_5)$ calculated values for phenothiazine radical cation (2.060) and promazine radical cations (3.318) are in good agreement with the experimental values of 2.546 and 3.612, respectively. Clarke and co-workers[19] examined the conformational behavior of N-substituted phenothiazine radical cations with electron paramagnetic spectroscopy (EPR) and concluded the substituent effect is mostly a through-bond inductive effect and the $\alpha(N)/\alpha(H5)$ ratio may be interpreted in terms of the fold angle of the radicals in repsonse to the substituent type.[19] The relative value of this $\alpha(N)/\alpha(H_5)$ ratio for side chains attached with primary or secondary carbons is consistent with the steric requirements of these types of substituents (e.g., the more hindered the aminum center the greater the fold induced in the heterocycle). Thus, the combination of the DFT-calculated optimized structure and hfcc's for the promazine radical cation indicate that it has a nonplanar ground electronic state.

TABLE 4: Spin Density Dsitributions for the Radical Cations of Phenothiazine (PTH) and Promazine (PRZ) Calculated Using DFT Methods with a 6-31G* Basis Set

	DFT/B3LYP calcd	
parameter	PTH	PRZ
ρ_S	0.2703	0.234
ρ_N	0.2577	0.326
ρ_{C1}	0.0215	0.0405
ρ_{C2}	0.0420	−0.0074
ρ_{C3}	0.116	0.122
ρ_{C4}	−0.054	−0.063
ρ_{C5}	0.105	0.110
ρ_{C6}	0.0017	−0.0017
ρ_{C8}	0.116	0.127
ρ_{C9}	0.042	0.001

Each hfcc is directly proportional to spin density at the hydrogen nucleus.[34] In Table 4, we present the spin densities on the carbon, sulfur, and nitrogen atoms of the promazine and phenothiazine radical cations derived using Mulliken population analysis with DFT (B3LYP) results. Due to the particular way of dividing spin density shared between atoms, Mulliken population analysis gives atomic charges and spin densities that are noticeably dependent on the particular basis set and computational method used.[35] However, calculated spin densities for the radical cations of promazine and phenothiazine in Table 4 show interesting qualitative features. The largest spin density is found at N (0.326) for promazine and at S (0.2703) for phenothiazine. It is interesting to note that the spin density at S (0.234) is a factor of 1.4 times smaller than the spin density at N. In addition, the values of the spin densities at C_3 (0.122) and C_8 (0.127) are larger than those of the other carbon atoms. This is consistent with EPR experimental results that suggest the side chain effect of promazine shows strong preferences for particular conformations along the C−N bond. Our DFT-calculated C−S and C−N bond lengths (1.762 and 1.407 Å, respectively) are noticeably shorter than corresponding DFT results for the neutral promazine molecule (1.778 and 1.416 Å, respectively). Similarly, the CSC and CNC bond angles increase significantly in the radical cation (101.13° and 124.84°, respectively) compared to the neutral promzaine molecule (99.29° and 121.68°, respectively).

Figure 2A presents the FT-Raman spectrum of promazine in its ground electronic state, and Table 5 compares experimental

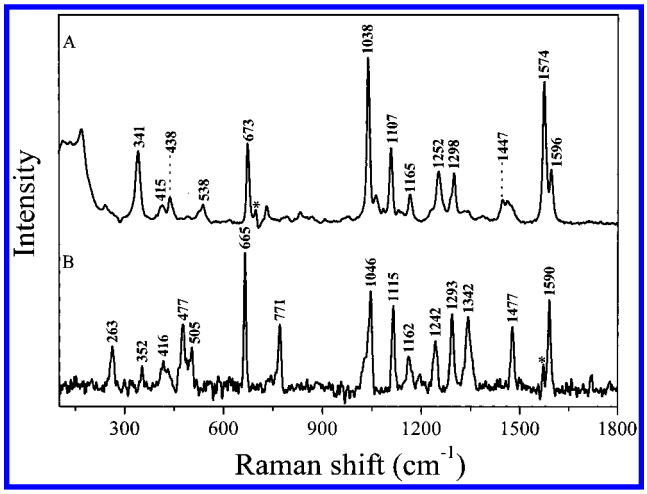

Figure 2. (A) FT-Raman spectrum obtained for neutral promazine molecule in the solution phase. The spectrum has been solvent and background subtracted. The asterisk marks a solvent subtraction artifact and the larger Raman bands are labeled with the value of their Raman shift in cm^{-1}. (B) Time-resolved resonance Raman spectrum of the radical cation of pomazine in the solution phase. The spectrum has been solvent and background subtracted, and the larger Raman bands are marked with their Raman shift wavenumber.

Raman vibrational frequencies with the RHF and DFT/B3LYP calculated vibrational frequencies (only Raman-active vibrational frequencies are given) for promazine. Table 5 also shows the DFT/B3LYP calculated isotopic shifts for S^{34}- and N^{15}-substituted promazine derivatives. The RHF-calculated vibrational frequencies have been uniformly scaled by 0.893 in Table 5 and appear reasonably close to experimental vibrational frequencies for the low-frequency modes and the higher frequency ring C−C modes but do not agree very well for most other higher frequency modes. In contrast, the DFT/B3LYP-calculated vibrational frequencies do not need any scaling and exhibit reasonable agreement with most of the experimental vibrational frequencies. Similar results have been observed in comparisons of HF and DFT ab initio computations for other organic molecular systems.[29,36] The DFT calculations include electron correlation effects and would be expected to give more accurate vibrational frequencies. One can use scaling factors for DFT-calculated vibrational frequencies to modestly improve the agreement with experimental values, although the scaling factors typically used[37,38] are close to one. This suggests that one may achieve reasonable agreement between the calculated DFT values and experimental frequencies without scaling, as shown here and for several other medium-sized organic molecular systems.[29,36] Similar DFT investigations of aromatic organic molecules showed that the ring C−C stretch and C−H stretch calculated frequencies scaled by ∼0.97−0.98 gave better agreement with the experimental values for these modes.[39] Our results also exhibit a similar larger discrepancy between the DFT-calculated frequencies and the experimental values for the ring C−C stretch and C−H modes. We can use a moderate amount of scaling (0.973 for the ring C−C stretch and C−H stretch modes, and the scaled values are shown in parentheses in Tables 5 and 6) to noticeably improve the agreement between the experiment and DFT-computed values.

The DFT/B3LYP calculations indicate the ring C−C stretch modes are at 1619 and 1641 cm^{-1}, and the experimental Raman bands at 1576 and 1596 cm^{-1} can be easily assigned to these two modes, which is similar to our previous assignments for the phenothiazine molecule.[18] The experimental bands at 1447 and 1460 cm^{-1} are assigned to the DFT-calculated 1433 cm^{-1} (CH_2 wag) and 1484 cm^{-1} (CH_3 sym def) vibrational modes, while the bands at 1385 and 1341 cm^{-1} are assigned to CH_2 twist modes and the 1298 cm^{-1} band is assigned to the CH_2 twist + C−H bend mode at 1301 cm^{-1}. The C−N−C symmetric stretch mode with a DFT-calculated frequency of 1283 cm^{-1} is assigned to the experimental 1252 cm^{-1} Raman band based on comparison to the analogous mode in phenothiazine[18] and chlorpromazine.[40] The C−S−C symmetric stretch symmetric vibrational mode (DFT-calculated frequency of 1127 cm^{-1}) is assigned to the experimental band at 1107 cm^{-1}. We note that the DFT/B3LYP-calculated isotopic shifts upon ^{34}S and ^{15}N substitutions for the C−S−C and C−N−C symmetric stretch modes are very similar to the experimental isotopic shifts observed for the corresponding modes in the phenothiazine molecule (as reported by Takahashi and co-workers[20]). The band at 1038 cm^{-1} is assigned to either the ring breathing or $C-N_{18}$ stretch modes (DFT values at 1074 and 1062 cm^{-1}, respectively). The bands at 415 and 438 cm^{-1} are assigned to the $CN_{10}C$ wag and CSC bend vibrational modes, respectively. The experimental 673 cm^{-1} Raman band is assigned to the $CN_{10}C$ bend or the CCC bend vibrational modes. The DFT calculation results and their correspondence to the experimental Raman bands were used to make preliminary assignments (shown in Table 5) for the other experimentally observed Raman bands. Figure 3 shows the DFT-calculated internal coordinate contributions to each of the normal modes tentatively assigned to the experimentally observed Raman bands for the neutral promazine molecule. We note some caveats about our preliminary vibrational assignments for the promazine molecule. For medium sized molecules, such as promazine, it is difficult to unambiguously assign some vibrational modes using DFT computations when several different modes have calculated frequencies within a range smaller than the typical error limits of the computation and the uncertainties of the experiments. For example, it is not clear whether the experimental 673 cm^{-1} Raman band should be assigned to the DFT-calculated $CN_{10}C$ bend frequency of 658 cm^{-1} or the CCC bend frequency of 693 cm^{-1}. However, the $^{15}N_{10}$-substituted promazine Raman band would allow us to clearly make the assignment since the $CN_{10}C$ bend frequency shifts by 5 cm^{-1} but the CCC bend frequency stays the same. This illustrates the utility of using isotopic vibrational band frequency shifts to help improve the vibrational assignments in medium-sized molecules such as promazine. We are not equipped to make the ^{34}S and ^{15}N isotopic derivatives of promazine in our laboratory, but we have listed the DFT-calculated isotopic shifts expected for the different promazine normal modes in Table 5. These calculated isotopic shifts can be compared to corresponding experimental data when they become available to improve our preliminary vibrational assignments for the promazine molecule (and the radical cation of promazine). Since our vibrational assignments for promazine are generally consistent with those previously made for the structurally similar phenothiazine molecule,[18] which does have ^{34}S- and ^{15}N-substituted isotopic experimental data available,[20] we are reasonably confident in the preliminary vibrational assignments presented for promazine in Table 5.

Figure 2B shows a time-resolved resonance Raman spectrum of the radical cation of promazine. Table 6 presents a comparison of the UHF- and DFT/B3LYP-calculated vibrational frequency with the experimental resonance Raman band frequencies for the promazine radical cation shown in Figure 1B. The DFT/B3LYP-calculated vibrational frequencies generally display reasonable agreement with the experimental Raman band frequencies for the promazine radical cation in Table 6. The

TABLE 5: Vibrational Frequencies of the Neutral Promazine Molecule Calculated Using HF and DFT/B3LYP Methods with a 6-31G* Basis Set; Calculated Frequencies Compared to Experimental Values Where Available

approximate description	calcd RHF	calcd DFT[b]	expt[a]	^{34}S subst DFT	$^{15}N_{10}$ subst DFT	$^{15}N_{18}$ subst DFT
central ring def (out-of-plane butterfly like mode)	59	58				
central ring boat def	76	84				
ring def (out of plane)	105	107	112 w			
central ring boat def	170	175	170 s	1.1	1	1
$N_{10}CCC$ torsion	225	233				
ring def (out of plane)	237	241	242 w			
CSC wag	272	283		1.8	1.5	
ring def (out of plane)	330	340	341 vs			
ring def (out of plane)	335	379				
$CN_{10}C$ wag	375	401	415 w	1	5.2	
$CN_{18}C$ wag	384	392				7.7
CSC bend	433	451	438 m	2.4	1.7	
Ring def (out of plane)	469	488	492 vw			
central ring def	508	518	538 m	2.3	2.8	
$CN_{10}C$ bend + CCC bend	614	634			3	
$CN_{10}C$ bend	634	658	673 vs ?		5	
CCC bend	672	693	673 vs ?			
ring def (in the plane)	689	712		1	1.9	
CH_2 rock	713	739	731 m			
C−H bend (out of plane)	749	754				
C−H bend (out of plane)	763	779				
C−H bend (out of plane)	777	784	795 vw			
$N_{10}C_{15}C_{16}$ wag	805	838	834 vw		2.4	
$C_{15}C_{16}$ stretch + CH_2 rock	847	886	870 vw		7	
CH_2 rock + CH_2 twist	877	909	907 vw			
C−H bend (out of plane)	908	961				
C−H bend (out of plane)	998	1006	974 vw			
C−N_{18} stretch	1026	1062	1038 vs ?			6.2
ring breathing	1030	1074	1038 vs ?		1.8	
C−H bend	1057	1083	1084 vw			
CSC sym stretch	1092	1127	1107 s	1	5	
CH_3 wag	1102	1139	1131 vw			
C−H bend	1126	1175	1165 m			
C−H bend	1140	1189			1.4	
CH_2 twist	1171	1208				4.4
C−H bend	1216	1233				
CH_2 twist	1221	1260	1252 s ?			6
$CN_{10}C$ sym stretch	1244	1283	1252 s ?		9	
CH_2 twist + C−H bend	1256	1301	1298 s			
CH_2 twist + C−H bend	1293	1330				
CH_2 twist	1310	1348	1341 vw			
CH_2 twist	1347	1386	1385 vw			
$CN_{10}C$ asym stretch	1367	1412			12	
CH_2 wag	1384	1422				
CH_2 wag	1394	1433	1447 m			
CH_3 sym. def	1436	1484	1460 m			
C−H bend	1449	1497				
CH_3 sym stretch	1459	1507				
CH_3 bend	1473	1526				
CH_3 bend + CH_2 bend	1480	1535				
CH_2 bend	1492	1549				
CH_2 bend	1501	1566				
ring CC stretch	1576	1619 (1575)	1574 vs			
ring CC stretch	1593	1634 (1590)				
ring CC stretch	1602	1660 (1615)	1596 s			
CH_3 sym stretch	2780	2931 (2852)				
CH_2 sym stretch	2790	2946 (2866)				
CH_2 asym stretch	2872	3066 (2983)				
CH_2 sym stretch	2881	3074 (2991)				
CH_3 asym stretch	2895	3092 (3008)				
CH_2 asym stretch	2917	3108 (3024)				
CH_2 asym stretch	2934	3129 (3044)				
C−H asym stretch	3000	3197 (3110)				
C−H asym stretch	3012	3207 (3120)				
C−H sym stretch	3030	3228 (3141)				
C−H stretch	3084	3267 (3179)				

[a] This work. Experiment intensity description: vs = very strong; s = strong; m = medium; w = weak; vw = very weak. [b] DFT calculated values in parentheses are ring C−C stretch and C−H stretch frequencies scaled by 0.973 (see text).

experimental Raman bands ~1590 cm^{-1} are assigned to the ring C−C stretch modes (DFT-calculated 1634 and 1616 cm^{-1}). The bands at 1342 and 1293 cm^{-1} are assigned to the CH_2 twist and $CN_{18}C$ asymmetric stretch modes (DFT-calculated 1338 and

TABLE 6: Vibrational Frequencies of the Radical Cation of Promazine Calculated Using HF and DFT/B3LYP Methods with a 6-31G* Basis Set; Calculated Frequencies Compared to Experimental Values Where Available

approximate description	calcd RHF	calcd DFT[b]	expt[a]	^{34}S subst DFT	$^{15}N_{10}$ subst DFT	$^{15}N_{18}$ subst DFT
central ring def (out-of-plane butterfly like mode)	61	60				
ring def (out of plane)	83	91				
ring def (out of plane)	99	110				
central ring boat def	160	178				
ring def (out of plane)	215	233				
central ring boat def	263	277	263 m			
ring def (out of plane)	328	348	352 w			
$CN_{10}C$ wag	406	412	416 w		4.2	
CSC bend	436	464	477 s	7.3		
$N_{10}CC$ wag	454	489	505 m			
CCC bend	591	628				
$CN_{10}C$ bend	633	658	665 vs ?		10	
ring def	640	687	665 vs ?	7	9	9
C−H bend (out of plane)	713	750				
C−H bend (out of plane) + $C_{15}-N_{10}$ stretch	736	784	771 s			
C−H bend (out of plane)	745	796				
C−H bend (out of plane)	759	805				
CH_2 rock	811	842				
C−H bend (out of plane)	844	896				
CH_2 rock	854	912				
C−H bend (out of plane)	870	924				
C−H bend (out of plane) + $C_{16}-C_{17}$ stretch	949	994				
ring def + $C_{15}-N_{10}$	961	1042	1046 vs ?			
$CN_{18}C$ sym stretch	1017	1050	1046 vs ?			10
ring breathing	976	1063				
C−H bend	1035	1091				
CH_2 rock + CH_3 twist	1043	1113				
CSC sym stretch	1062	1121	1115 vs	2	1	
C−H bend	1084	1176				
CH_3 wag	1099	1132				
C−H bend	1117	1176	1162 m			
C−H bend + CH_2 twist	1130	1201				
C−H bend	1168	1211				
C−H bend	1179	1233				
CH_2 twist	1195	1252	1242 s ?			
$CN_{10}C$ sym stretch	1161	1263	1242 s ?	1	6	1
$CN_{18}C$ asym stretch	1277	1299	1293 s			8.4
CH_2 twist	1264	1338	1342 s			
C−H bend	1233	1354				
$CN_{10}C$ asym stretch	1321	1395			8	1
CH_2 wag	1337	1383				
CH_2 wag	1369	1411				
CH_2 wag	1389	1428				
C−H bend	1412	1490	1477 s			
C−H bend	1421	1501				
CH_3 sym def	1438	1508				
C−H bend	1456	1513				
CH_3 bend	1473	1527				
CH_3 bend + CH_2 bend	1481	1546				
CH_2 bend	1486	1589				
ring CC stretch	1494	1616 (1572)				
ring CC stretch	1543	1634 (1589)	1590 vs			
CH_3 sym stretch	2816	2979 (2898)				
CH_2 sym stretch	2831	2991 (2910)				
CH_2 sym stretch	2883	3069 (2986)				
CH_2 asym stretch	2891	3083 (2999)				
CH_3 asym stretch	2904	3101 (3017)				
CH_2 asym stretch	2925	3112 (3027)				
CH_3 asym stretch	2941	3141 (3056)				
CH_2 asym stretch	2963	3170 (3084)				
C−H asym stretch	3023	3222 (3135)				
C−H asym stretch	3030	3232 (3145)				
C−H sym stretch	3055	3249 (3161)				
C−H stretch	3092	3286 (3197)				

[a] This work. [b] DFT calculated values in parentheses are ring C−C stretch and C−H stretch frequencies scaled by 0.973 (see text).

1299 cm^{-1}, respectively). The 1242 cm^{-1} experimental Raman band is assigned to the $C-N_{10}-C$ symmetric stretch mode (DFT-calculated frequency of 1263 cm^{-1}) or the CH_2 twist mode (DFT mode at 1252 cm^{-1}). The experimental 1115 cm^{-1} band

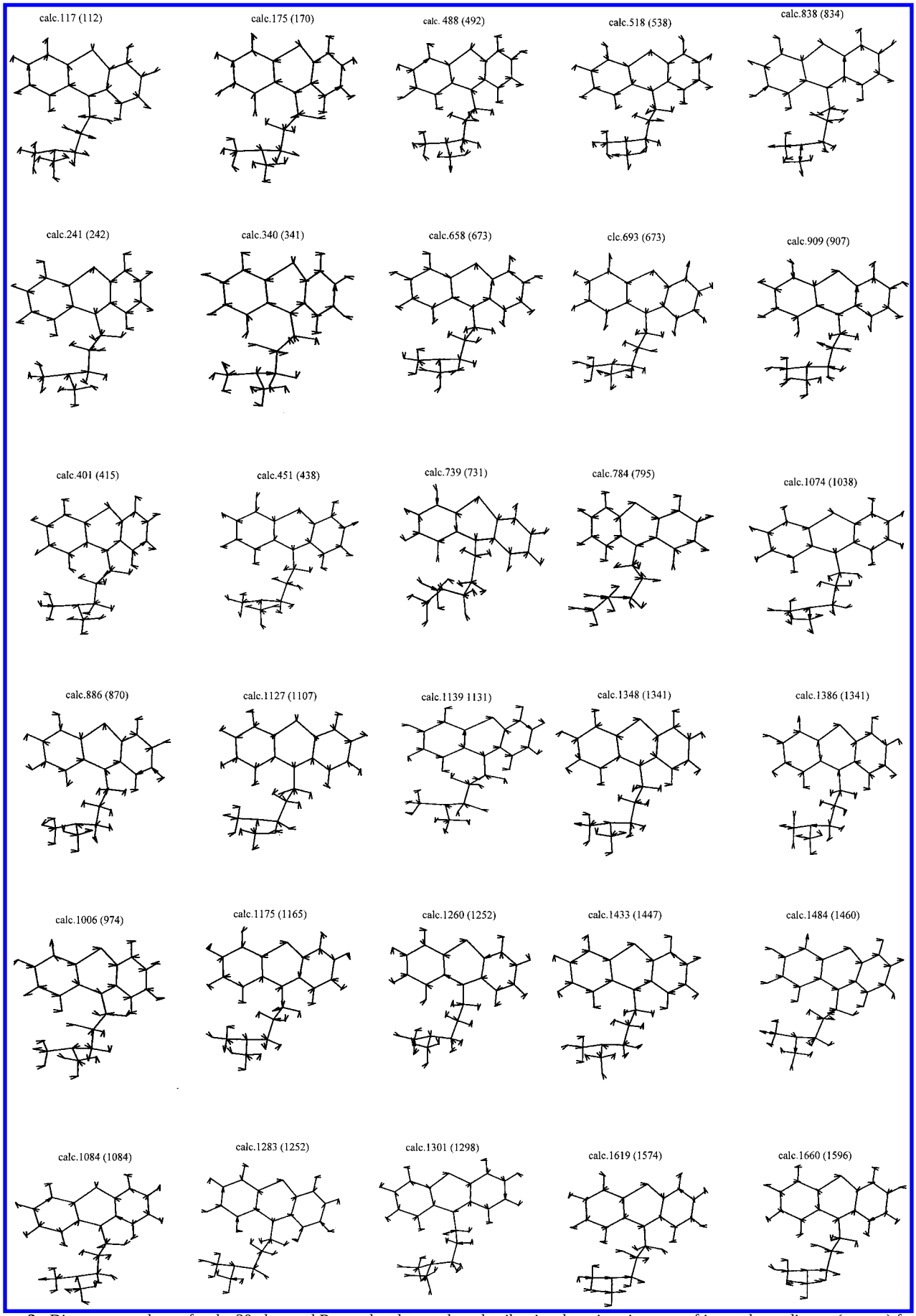

Figure 3. Diagrams are shown for the 30 observed Raman band normal mode vibrational motions in terms of internal coordinates (arrows) for the neutral promazine molecule. Each diagram is labeled with the DFT calculated vibrational frequency and its experimental value (in cm^{-1}) as listed in Table 5.

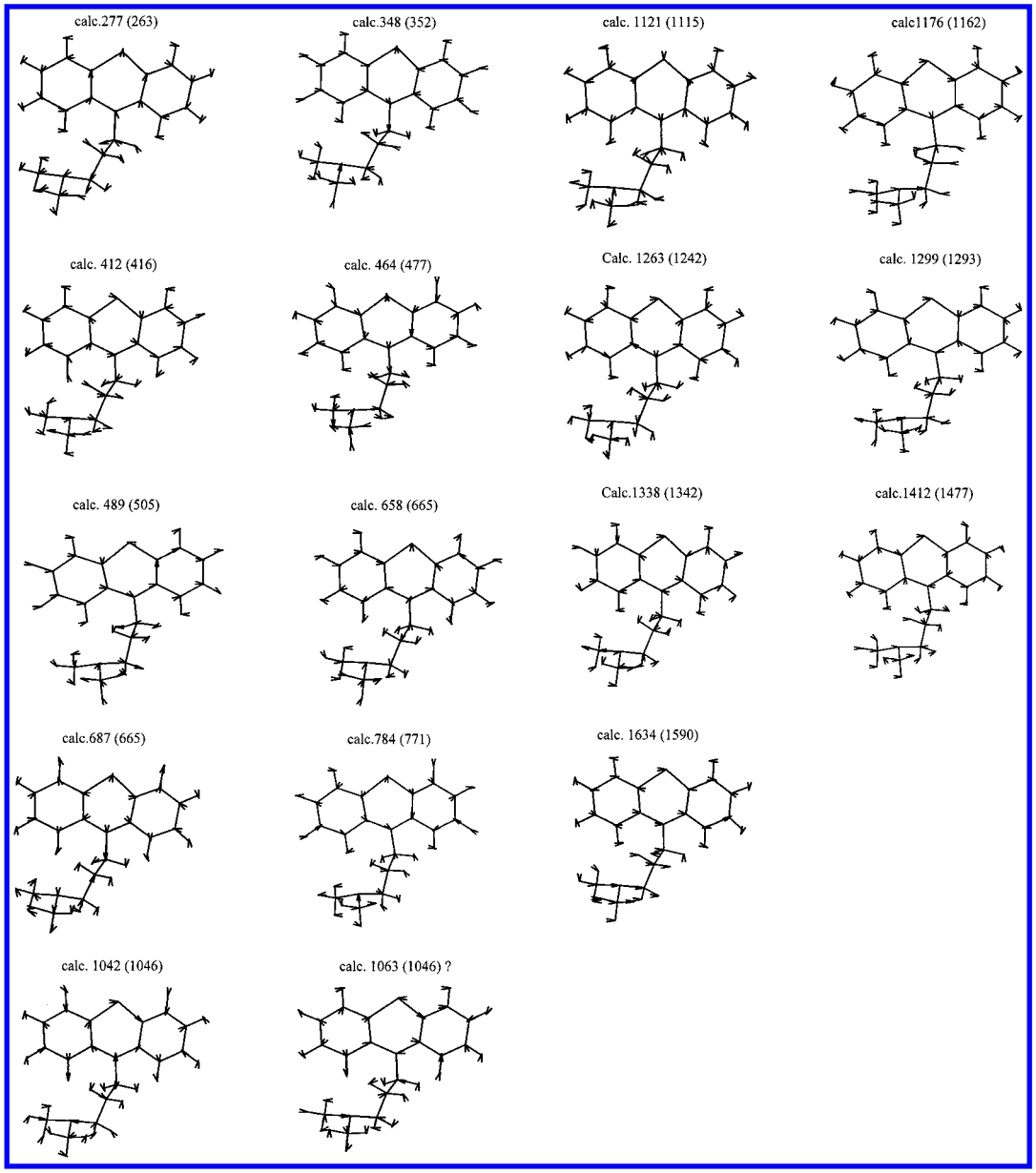

Figure 4. Diagrams are shown for 17 observed Raman band normal mode vibrational motions in terms of internal coordinates (arrows) for the radical cation of promazine. Each diagram is labeled with the DFT calculated vibrational frequency and its experimental value (in cm^{-1}) as listed in Table 6.

is assigned to the C−S−C symmetric stretch mode (DFT-calculated frequency of 1121 cm^{-1}). The 1046 cm^{-1} Raman band is tentatively assigned to the $CN_{18}C$ symmetric stretch or ring def + $C_{15}-N_{10}$ stretch modes (DFT-calculated 1050 and 1042 cm^{-1}, respectively). Similarly, the 665 cm^{-1} Raman band is tentatively assigned to the ring def or the $CN_{10}C$ bend modes (DFT-calculated 687 and 658 cm^{-1}, respectively). The experimental 771, 505, 477, and 416 cm^{-1} bands are assigned to the C−H bend (out of plane) + $C_{15}N_{10}$ stretch, $N_{10}CC$ wag, CSC bend, and $CN_{10}C$ wag vibrational modes (DFT-calculated at 784, 489, 464, and 412 cm^{-1} respectively). The lower frequency Raman bands at 263 and 352 cm^{-1} are assigned to the central ring boat deformation and ring deformation (out of plane) vibrational modes (DFT-calculated at 277 and 348 cm^{-1}, respectively). Figure 4 shows the DFT-calculated internal coordinate contributions to each of the normal modes tentatively assigned to the experimentally observed Raman bands for the promazine radical cation.

Figure 5 displays a simple diagram of the promazine and phenothiazine which can be referred to when we compare these molecules and their radical cations. The vibrational frequencies of the CSC bend and CSC symmetric stretch modes increase from 438 and 1105 cm^{-1} in the neutral promazine molecule to 477 cm^{-1} (a +38 cm^{-1} shift) and 1115 cm^{-1} (a 8 cm^{-1} shift) in its radical cation. This suggests that the dihedral angle of the radical cation along the S−N axis becomes greater than that of the parent neutral molecule. This is consistent with the results of both HF and DFT calculations and EPR experiments for promazine and X-ray experiments for chlorpromazine (see Tables 1 and 2). Photoelectron spectra results also suggest that the dihedral angle change upon formation of the radical cation produces better π-orbital overlap between the C−N atoms as well as the ring C and S atoms to give larger aromatic resonance stabilization of the radical cation structure that affects the C−C and C−N bonds electron density compared to the two phenyl rings. Inspection of Tables 5 and 6 shows that the phenyl ring CC stretch, ring breathing, and C−H bending modes do not change much in going from the neutral promazine molecule to the radical cation. The experimental CNC symmetric stretch mode in phenothiazine[18] increases from 1243 cm^{-1} in the neutral

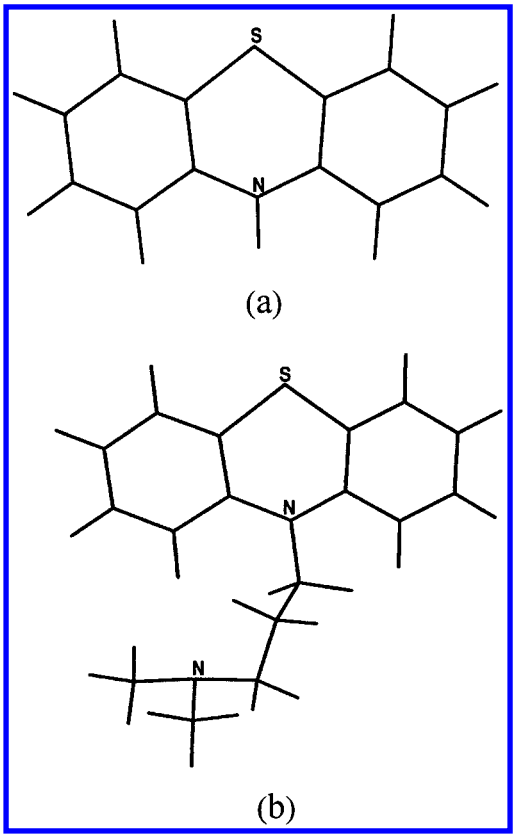

Figure 5. Diagram of the geometries of phenothiazine and promazine.

molecule to 1267 cm^{-1} in the radical cation (a +24 cm^{-1} shift). However, the corresponding $CN_{10}C$ symmetric stretch mode in promazine decreases in frequency from 1252 cm^{-1} (DFT frequency of 1283 cm^{-1}) in the neutral molecule to 1242 cm^{-1} (DFT frequency of 1263 cm^{-1}) in the radical cation (a −10 cm^{-1} experiment shift or −20 cm^{-1} calculated shift). In contrast, the $CN_{10}C$ bend mode remains similar in the neutral promazine and the radical cation (experiment 673 cm^{-1} in promazine to 665 cm^{-1} in the radical cation or DFT-calculated 658 cm^{-1} in both promazine and the radical cation). The lack of frequency upshifts for the $CN_{10}C$ mode upon oxidation for promazine suggests that the promazine radical cation still contains some fold angle and a nonplanar structure, in contrast to the phenothiazine radical cation which is planar.[18] This is consistent with the DFT-calculated dihedral angle of 172°, the calculated $\alpha(N)/\alpha(H_5)$ ratio and experimental EPR spectra.[11,12] It is interesting to note that the side chain $CN_{18}C$ asymmetric stretch mode and the $CN_{18}C$ symmetric stretch modes appear to have significant intensity in the radical cation resonance Raman spectra (Figure 2B), and this suggests that the side chain group perturbs the ring structure near the N_{10} atom and likely accounts for the frequency downshifts of the $CN_{10}C$ modes upon oxidation in promazine. Our Raman data and DFT calculations are consistent with the side chain group of promazine affecting the ring structure so that the promazine radical cation is significantly nonplanar in structure in contrast to the phenothiazine radical cation that is planar in structure.

There is a very interesting pattern in the C_2N_{10}, C_8N_{10}, $N_{10}C_{15}$, $C_{15}C_{16}$, $C_{16}C_{17}$, $C_{17}N_{18}$, $N_{18}C_{19}$, and $N_{18}C_{19}$ bond length changes upon oxidation of the promazine molecule to form the radical cation. Inspection of Tables 1 and 2 shows that these bond lengths change as follows: C_2N_{10} (−0.007 Å), C_8N_{10} (−0.009 Å), $N_{10}C_{15}$ (+0.030 Å), $C_{15}C_{16}$ (−0.001 Å), $C_{16}C_{17}$ (+0.006 Å), $C_{17}N_{18}$ (−0.001 Å), $N_{18}C_{19}$ (+0.008 Å), and $N_{18}C_{19}$ (+0.009 Å). As the two ring C_2N_{10} (−0.007 Å) and C_8N_{10} (−0.009 Å) bonds become shorter and stronger, the $N_{10}C_{15}$ (+0.030 Å) bond becomes noticeably longer and weaker and there is some alternation of bond length changes in the side chain group reminiscent of conjugation of the side chain with the increased aromaticity of the center ring containing the N_{10} and S atoms. This suggests that the $-(CH_2)_3N(CH_3)_2$ side chain interacts electronically (probably with a combination of conjugation and inductive through-bond effects) with the center ring containing the N_{10} and S atoms upon oxidation of the promazine molecule. This may also help explain why the promazine radical cation contains a much larger spin density on the N atoms relative to the S atom compared to the phenothiazine radical cation (see Table 4).

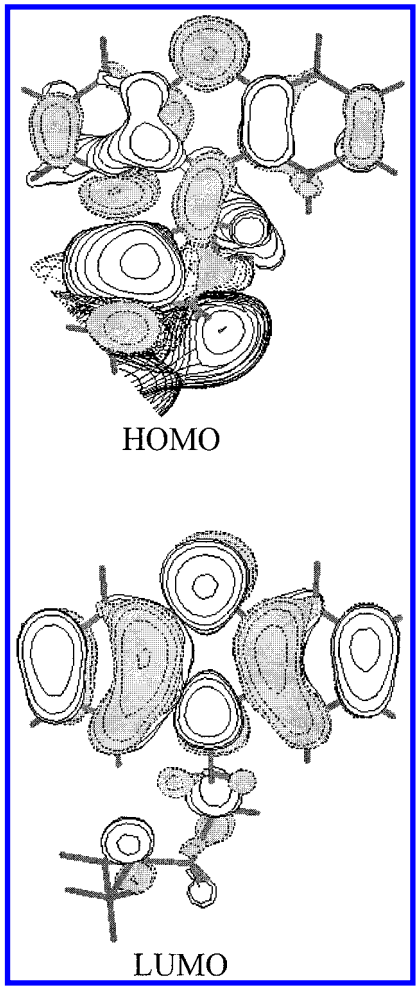

Figure 6. DFT calculated HOMO and LUMO electron density for the radical cation of promazine. The contour number is ±0.05.

We have calculated the electron density for the HOMO and LUMO of the promazine radical cation using both UHF and DFT methods. The calculated LUMO is the same for both the UHF and DFT calculations. However, the HOMO calculated for the DFT/B3LYP method corresponds to the second highest occupied molecular orbital (HOMO-1) calculated for the UHF method. This energy change is mainly due to the different level of theory used in the calculations. The hybrid HF/DFT (B3LYP) calculations consider the effect of electron correlation, but this is neglected in the HF method. Thus, the DFT methods tend to give a smaller HOMO−LUMO energy gap.[41] Since the DFT/B3LYP calculation includes electron correlation effects and is expected to be more accurate, we show these HOMO and LUMO electron densities in Figure 6 with a contour number of

0.025. Inspection of Figure 6 shows that the HOMO is localized not only on S but also on N_{10} and C_{15}, and this is consistent with the side chain of promazine affecting the spin density pattern and having preferences for particular conformations along the C−N bond. Inspection of the HOMO and LUMO in Figure 6 suggests that there are large changes along the side chain as well as the central ring. This is consistent with the resonance Raman spectrum of the radical cation of promazine which has a significant amount of the intensity appearing in the $CN_{10}C$ bend and/or ring def (665 cm^{-1}), CSC bend (477 cm^{-1}), C−H bend + $C_{15}N_{10}$ stretch (771 cm^{-1}), ring def + $C_{15}N_{10}$ stretch and/or $CN_{18}C$ sym stretch (1046 cm^{-1}), CSC sym stretch (1115 cm^{-1}), $CN_{10}C$ sym stretch and/or CH_2 twist (1242 cm^{-1}), and $CN_{18}C$ asym. stretch (1293 cm^{-1}) modes associated with the side chain and central ring.

Conclusion

We have reported a resonance Raman spectrum of the radical cation of promazine. Ab initio calculations were done for the ground electronic states of the neutral promazine molecule and its radical cation in order to elucidate the structures, hyperfine coupling constants (hfcc's), spin densities, and vibrational frequencies. We have made tentative assignments for all of the observed Raman bands for the neutral promazine molecule and its radical cation. We also calculated the vibrational frequency shifts associated with several isotopic derivatives of the neutral and radical cation of promazine. These can be used in conjunction with experimental data when they are available to help improve the vibrational band assignments. The DFT-calculated optimized structures indicate that the S_0 states of the neutral moleule (with a dihedral angle of 147.1°) and its radical cation (with a dihedral angle of 172.13°) are both nonplanar, and the calculated results display reasonable agreement with X-ray crystal data where available. The DFT-calculated hfcc's for the radical cations of phenothiazine and promazine are in good agreement with experimental values derived from ESR experiments. The DFT-calculated spin densities indicate that the radical cation of promazine has significantly more spin density on nitrogen compared to sulfur, while the sulfur has a greater spin density than nitrogen in the radical cation of phenothiazine. The DFT-calculated HOMO and LUMO electron densities indicate significant changes in both the central ring and the side chain upon excitation, and this appears consistent with the intensities found in the resonance Raman spectrum of the radical cation.

Acknowledgment. This work was supported by grants from the Committee on Research and Conference Grants (CRCG), the Research Grants Council (RGC) of Hong Kong, the Hung Hing Ying Physical Sciences Research Fund, and the Large Items of Equipment Allocation 1993−1994 from the University of Hong Kong. The authors thank Dr. X. J. Wang for his assistance with the calculations.

References and Notes

(1) Henry, B. R.; Kasha, M. *J. Chem. Phys.* **1967**, *47*, 3319−3327.
(2) Usdin, E.; Eckert, H.; Forrest, I. S. *Developments in Neuroscience*; Elsevier North-Holland: Amsterdam, 1980; Vol. 7.
(3) Alkalis, S. A.; Beck, G.; Grätzel, M. *J. Am. Chem. Soc.* **1975**, *97*, 5723−5729.
(4) Hu, M.; Kevan, L. *J. Phys. Chem.* **1990**, *94*, 5348−5351.
(5) Delay, J.; Deniker, P.; Harl, J. M. *Ann. Med. Psychol.* **1952**, *2*, 111−117.
(6) Bloor, J. E. *J. Med. Chem.* **1970**, *13*, 922−925.
(7) Foster, R. *Organic Charge-Transfer Complexes*; Academic Press: New York, 1969.
(8) Swarta, H. M.; Bolton, J. R.; Boog, D. C. *Biological Applications of Electron Spin Resonance*; Wiley-Interscience: New York, 1972.
(9) Gooley, C. M.; Keyzer, H.; Setchel, F. *Nature* **1969**, *223*, 80−83.
(10) Domelsmith, N. L.; Munchausen, L. L.; Houk, K. N. *J. Am. Chem. Soc.* **1977**, *99*, 6506−6514.
(11) López Rupérez, F.; Conesa, J. C.; Soria, J.; Apreda, M. C.; Cano, F. H.; Foces-Foces, C. *J. Phys. Chem.* **1985**, *89*, 1178−1182.
(12) Rodgers, J. R.; Horn, A. S.; Kennard, O. *J. Pharm. Pharacol.* **1976**, *28*, 246−247.
(13) Garcia, C.; Smith, G. A.; McGimpsey, W. M.; Kochevar, I. E.; Redmond, R. W. *J. Am. Chem. Soc.* **1995**, *117*, 10871−10878.
(14) Merville, M. P.; Pitte, J.; Lopez, M.; Decuyper, J.; Van de Vorst, A. *Photochem. Photobiol.* **1984**, *39*, 57.
(15) Nath, S.; Pal, H.; Palit, D. K.; Sapre, A. V.; Mittal, J. P. *J. Phys. Chem. A* **1998**, *102*, 5822−5830.
(16) McDowell, J. J. H. *Acta Crystallogr.* **1976**, *B32*, 5−10.
(17) Clarke, D.; Gilbert, B. C.; Hanson, P.; Kirk, M. C. *J. Chem. Soc., Perkin Trans.* **1978**, *2*, 1103−1110.
(18) Pan, D.-H.; Phillips, D. L. *J. Phys. Chem. A* **1999**, *103*, 4737−4743.
(19) Hester, R.; Williams, K. P. J. *J. Chem. Soc., Perkin II* **1981**, 852−858.
(20) Sarata, G. L.; Noda, Y.; Sakai, M.; Takahashi, H. J. *Mol. Struct.* **1997**, *413−414*, 49−59.
(21) Shoute, L. C. T.; Pan, D.-H.; Phillips, D. L. *Chem. Phys. Lett.* **1998**, *290*, 24−28.
(22) Pan, D.-H.; Shoute, L. C. T.; Phillips, D. L. *Chem. Phys. Lett.* **1998**, *292*, 677−685.
(23) Pan, D.-H.; Shoute, L. C. T.; Phillips, D. L. *Chem. Phys. Lett.* **1999**, *303*, 629−635.
(24) (a) Frisch, M. J.; Trucks, G. W.; Schlegel, H. B.; Gill, P. M. W.; Johnson, B. G.; Robb, M. A.; Cheeseman, J. R.; Keith, T. A.; Petersson, G. A.; Montgomery, J. A.; Raghavachari, K.; Al-Laham, M. A.; Zakrzewski, V. G.; Ortiz, J. V.; Foresman, J. B.; Cioslowski, J.; Stefanov, B. B.; Nanayakkara, A.; Challacombe, M.; Peng, C. Y.; Ayala, P. Y.; Chen, W.; Wong, M. W.; Andres, J. L.; Replogle, E. S.; Gomperts, R.; Martin, R. L.; Fox, D. J.; Binkley, J. S.; Defrees, D. J.; Baker, J.; Stewart, J. P.; Head-Gordon, M.; Gonzalez, C.; Pople, J. A. *Gaussian 94*, revision A.1; Gaussian Inc.: Pittsburgh, PA, 1995. (b) Frisch, M. J.; Trucks, G. W.; Schlegel, H. B.; Scuseria, G. E.; Robb, M. A.; Cheeseman, J. R.; Zakrzewski, V. G.; Montgomery, J. A.; Stratmann, R. E.; Burant, J. C.; Dapprich, S.; Millam, J. M.; Daniels, A. D.; Kudin, K. N.; Strain, M. C.; Farkas, O.; Tomasi, J.; Barone, V.; Cossi, M.; Cammi, R.; Mennucci, B.; Pomelli, C.; Adamo, C.; Clifford, S.; Ochterski, J.; Perterson, G. A.; Ayala, P. Y.; Cui, Q.; Morokuma, K.; Mailick, D. K.; Rabuck, A. D.; Raghavachari, K.; Foresman, J. B.; Cioslowski, J.; Orvitz, J. V.; Stefanov, B. B.; Liu, G.; Liashenko, A.; Piskorz, P.; Komaromi, I.; Gomperts, R.; Martin, R. L.; Fox, D. J.; Kieth, T.; Al-laham, M.-A.; Peng, C. Y.; Nanayakkara, A.; Gonzalez, C.; Challacombe, M.; Gill, P. M. W.; Johnson, B. G.; Chen, W.; Wong, M. W.; Andres, J. L.; Head-Gordon, M.; Perlogle, E. S.; Pople, J. A. *Gaussian 98*, revision A.1; Gaussian, Inc.: Pittsburgh, PA, 1998.
(25) Becke, A. D. *J. Chem. Phys.* **1993**, *98*, 1372−1377.
(26) NMODES is a program that directly takes the Gaussian 94 or G98W output file and determines the normal modes and potential energy distributions in internal coordinates. The program was developed by P. Mohandas and, S. Umapathy, Indian Institute of Science, Bangalore, India, 1997.
(27) Schaftenaar, G. *MOLDEN*; CAOS/CAMM Center: The Netherlands 1991.
(28) Bell, J. D.; Blount, J. F.; Briscoe, O. V.; Freeman, H. C. *Chem. Commun.* **1968**, 1656−1657.
(29) Qin, Y.; Wheeler, R. A. *J. Phys. Chem.* **1996**, *100*, 10554−10563.
(30) López Rupérez, F.; Conesa, C. J.; Soria, J. *J. Mol. Struct.* **1983**, *98*, 165−174.
(31) Eriksson, L. A.; Malkina, O. L.; Malkin, V. G.; Salahub, D. R. *J. Chem. Phys.* **1994**, *100*, 5066−5075.
(32) Adamo, C.; Barone, V. *J. Phys. Chem.* **1994**, *98*, 8648−8652.
(33) Ishii, N.; Shimizu, T. *Phys. Rev. A* **1993**, *48*, 1691−1694.
(34) Weil, J.; Bolton, J. R.; Wertz, J. E. *Electron Paramagnetic Resonance*; Wiley-Interscience: New York, 1994.
(35) Mulliken, R. S.; Ermler, W. C. *Diatomic Molecules*; Academic: New York, 1977.
(36) Mohandas, P.; Umapathy, S. *J. Phys. Chem. A* **1997**, *101*, 4449−4459.
(37) Raouhut, G.; Pulay, P. *J. Phys. Chem.* **1995**, *99*, 3093−3100.
(38) Castella-Ventura, M.; Kassab, E. *J. Raman Spectrosc.* **1998**, *29*, 511−536.
(39) Gallouj, H.; Lagant, P.; Vergoten, G. *J. Raman Spectrosc.* **1998**, *29*, 343−351.
(40) Pan, D.; Shoute, L. C. T.; Phillips, D. L. *J. Phys. Chem.*, submitted.
(41) Foresman, J. B.; Frisch, A. E. *Exploring Chemistry with Electronic Structure Methods*, 2nd ed.; Gaussian, Inc.: Pittsburgh, 1996.